Uracil on Cu(110): A quantitative structure determination by energy-scanned photoelectron diffraction

D. A. Duncan, W. Unterberger, D. Kreikemeyer-Lorenzo, and D. P. Woodruff

Citation: The Journal of Chemical Physics **135**, 014704 (2011); doi: 10.1063/1.3607246
View online: http://dx.doi.org/10.1063/1.3607246
View Table of Contents: http://scitation.aip.org/content/aip/journal/jcp/135/1?ver=pdfcov
Published by the AIP Publishing

Uracil on Cu(110): A quantitative structure determination by energy-scanned photoelectron diffraction

D. A. Duncan,[1] W. Unterberger,[2] D. Kreikemeyer-Lorenzo,[2] and D. P. Woodruff[1,a)]
[1]*University of Warwick, Coventry, CV4 7AL, United Kingdom*
[2]*Fritz-Haber-Institut der MPG, Faradayweg 4-6, D 14195, Berlin, Germany*

(Received 21 April 2011; accepted 14 June 2011; published online 6 July 2011)

The local adsorption site of the nucleobase uracil on Cu(110) has been determined quantitatively by energy-scanned photoelectron diffraction (PhD). Qualitative inspection of the O 1s and N 1s soft x-ray photoelectron spectra, PhD modulation spectra, and O K-edge near-edge x-ray adsorption fine structure indicate that uracil bonds to the surface through its nitrogen and oxygen constituent atoms, each in near atop sites, with the molecular plane essentially perpendicular to surface and aligned along the close packed [1$\bar{1}$0] azimuth. Multiple scattering simulations of the PhD spectra confirm and refine this geometry. The Cu-N bondlength is 1.96 ± 0.04 Å, while the Cu–O bondlengths of the two inequivalent O atoms are 1.93 ± 0.04 Å and 1.96 ± 0.04 Å, respectively. The molecule is twisted out of the [1$\bar{1}$0]direction by 11 ± 5°. © *2011 American Institute of Physics*. [doi:10.1063/1.3607246]

I. INTRODUCTION

In recent years there has been growing interest in how amino acids and nucleobases, the constituents of biological compounds, interact with inorganic matter. Though these molecules are simple in the biological sense, they are comparatively complex for quantitative surface structural investigations. However, the elemental and chemical-state specificity of scanned-energy mode photoelectron diffraction (PhD),[1,2] combined with its essentially local character, make it well-suited to investigating such systems. On the Cu(110) surface, PhD has already been used to determine the adsorption geometry of the simple amino acids glycine[3,4] and alanine,[5] and two of the pyrimidine nucleobases, cytosine[6] and thymine.[7] In all four cases the molecules adsorb through their nitrogen and oxygen constituent atoms, which are singly coordinated to surface Cu atoms. In the case of the thymine, a molecule that closely resembles uracil, the subject of this study (see Fig. 1), the molecule adsorbs through the two carbonyl oxygen atoms and the deprotonated nitrogen (N(3)) atom between them - with all three atoms in local near-atop sites.

There have been rather few studies of uracil adsorption at surfaces at the solid-vacuum interface although the gold/uracil system has attracted significant interest in model electrochemical studies of nucleobase/metal surface interactions. At different applied potentials both physisorbed and chemisorbed species have been proposed, but while there have been several investigations using *in situ* STM (scanning tunnelling microscopy), no significant information regarding the adsorption geometry at the interface has emerged from most of these studies. However, while much of this work has been reviewed by Li *et al.*,[8] these authors, through the combination of STM and infrared spectroscopy, did identify a chemisorbed phase in which they concluded that uracil bonds through the N(3) atom (Fig. 1) and the two adjacent O atoms with its molecular plane perpendicular to the surface. This geometry is similar to the Cu(110)/thymine structure referred to above and is also consistent with our findings for Cu(110)/uracil reported here. The exact location of the chemisorbed uracil on the Au(111) surface was not, however, identified.

At the solid-vacuum interface there have been a few studies of the system studied here, uracil adsorption on Cu(110), but little resulting structural information. A brief report of a STM investigation of this system remarks only on the adsorbate-induced surface faceting that occurs at elevated temperatures.[9] Some limited structural information is provided by ARUPS (angle-resolved ultraviolet photoemission spectroscopy) data, which indicate that the molecular plane lies perpendicular to the surface, orientated along one of the substrate mirror symmetry planes.[10] A density functional theory (DFT) calculation of Cu-uracil complexes finds Cu–O bonding to be preferred over Cu-N bonding, with Cu–N and Cu–O bondlengths in the ranges 1.98–2.16 Å and 1.88–2.07 Å, respectively, depending on the ionisation state of the complex.[11] Here, we show that application of the PhD technique to this adsorption system provides a rather complete picture of the local adsorption geometry and allows us to compare the solution with that of related molecules on Cu surfaces.

II. EXPERIMENTAL DETAILS

The experiments were conducted in an ultra-high vacuum surface science end-station equipped with typical facilities for sample cleaning, heating, and cooling. This instrument was installed on the UE56/2-PGM-2 beam line of BESSY-II, which comprised a 56 mm period undulator followed by a plane grating monochromator.[12] The sample could be rotated about its surface normal (to change the azimuthal angle) and about its vertical axis (to change the polar angle), allowing (simultaneous) variation of incidence and

a)Author to whom correspondence should be addressed. Electronic mail: d.p.woodruff@warwick.ac.uk.

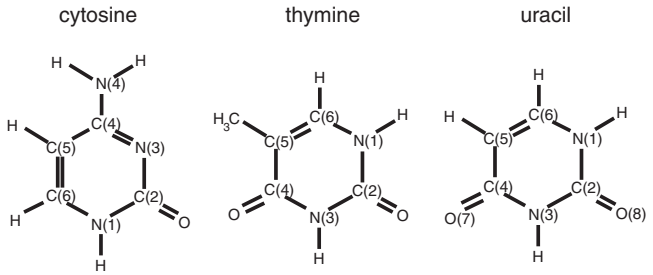

FIG. 1. Molecular structure of (a) cytosine, (b) thymine, and (c) uracil, showing the labelling convention for the constituent atoms. Note the similarity between the thymine and uracil molecules, only differing by a methyl group attached to C(5).

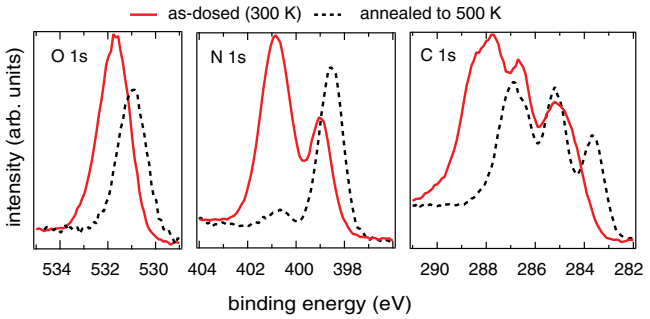

FIG. 2. Comparison of soft x-ray photoelectron spectra in the energy range of the (from top to bottom) O 1s, N 1s and C 1s emission peaks from uracil deposited on Cu(110) at room temperature, and after annealing to ∼500 K. The spectra were recorded at normal emission with photon energies of 650 eV, 500 eV, and 400 eV for the O 1s, N 1s, and C 1s regions, respectively. Absolute binding energies have been adjusted as described in the text.

electron collection directions. Sample characterisation *in situ* was achieved by LEED (low energy electron diffraction), and by SXPS (soft x-ray photoemission spectroscopy) using the incident synchrotron radiation. The SXPS, NEXAFS (near-edge x-ray absorption fine structure), and PhD measurements were obtained using an Omicron EA-125HR 125 mm mean-radius hemispherical electrostatic analyser. The analyser was equipped with seven-channeltron parallel detection, and was mounted at a fixed angle of 60° to the incident radiation, in the same horizontal plane as that of the polarisation vector of the radiation.

A clean, well-ordered Cu(110) surface was prepared from an oriented and polished crystal slice by the usual combination of Ar ion bombardment and brief annealing to 800 K, to give a sharp (1×1) LEED pattern and a SXP spectrum devoid of impurities. Uracil powder of 99+% purity was obtained from Alfa Aesar. During sample dosing the uracil was heated to 575 K, while the substrate was kept at room temperature. No ordered overlayer was observed by LEED. Based on a comparison of the O 1s and Cu 2p photoemission intensity ratio obtained from a Cu(110)(2×1)-O surface the uracil coverage of the surface studied was ∼0.25 ML.

The PhD modulation spectra were obtained by measuring photoelectron energy distribution curves (EDCs) of the O 1s and N 1s peaks, at 4 eV steps in photon energy, over the photoelectron kinetic energy range of 50–350 eV, for a number of different polar emission angles, θ, in the [001] and [1$\bar{1}$0] azimuths. These data were processed following our general PhD methodology (e.g., Refs. 1 and 2) in which the individual EDCs are fitted by a sum of Gaussian peaks, a Gauss error function, and a template background. The integrated areas of each of the individual chemically shifted component peaks were then plotted as a function of photoelectron kinetic energy, and used to define a smooth spline which represents the non-diffractive intensity and instrumental factors. The spline was then subtracted from, and used to normalise, the integrated areas, to provide the final PhD modulation spectrum.

O K-edge NEXAFS spectra were recorded in the Auger electron detection mode by measuring the intensity of the electron emission from the O KVV Auger transition at 513 eV while scanning through the photon energy. Spectra were recorded in the two high symmetry azimuths ([001] and [1$\bar{1}$0]) at two angles of incidence (normal (0°) and 60° polar angle). These changes in incidence geometry provide information on the dependence of the intensity of the molecular resonance peaks on the direction of the polarisation vector of the linearly polarised incident radiation, and provide the basis for a determination of the molecular orientation.

III. RESULTS

A. Characterisation by SXPS and NEXAFS

Figure 2 shows SXP spectra recorded around the O 1s, N 1s and C 1s core level photoemission peaks from uracil on Cu(110), immediately after deposition at room temperature, and after annealing to 500 K. Initial dosing with the surface at 500 K led to spectra identical to those obtained by annealing the lower-temperature deposited layers. While the room temperature deposited layer exhibits two chemically distinct N 1s components, annealing to 500 K leads to almost complete loss of one component and increase of the other, accompanied by a small energy shift. The O 1s spectra, on the other hand, show only a single peak under both conditions, although in this case, too, there is a shift in the peak energy following annealing. This behaviour is essentially identical to that seen for thymine on Cu(110) by both Furukawa *et al.*[13] and Allegretti *et al.*[7] Note that as we are primarily interested in relative peak energies and chemical shifts, no experimental absolute calibration of the binding energies was undertaken, but because of the close similarity of these uracil and thymine data our measured values (nominal photon energy minus measured kinetic energy) were adjusted to align the main peaks of the N 1s and O 1s spectra to those previously reported for adsorbed thymine. A similar interpolated energy shift has been applied to the C 1s spectra. The interpretation of the N 1s spectra proposed in the thymine studies was that one of the N atoms in the molecule is dehydrogenated upon adsorption, while heating to 500 K leads to dehydrogenation of the other N atom. For thymine on Cu(110) this second dehydrogenation step is supported by the results of temperature programmed desorption measurements that show H_2 desorption occurs at 463 K.[14,15] We therefore infer that similar dehydrogenation steps occur at similar temperatures for uracil on Cu(110). Notice that the higher binding energy component of N 1s spectrum from the as-dosed surface at 300 K seems to be

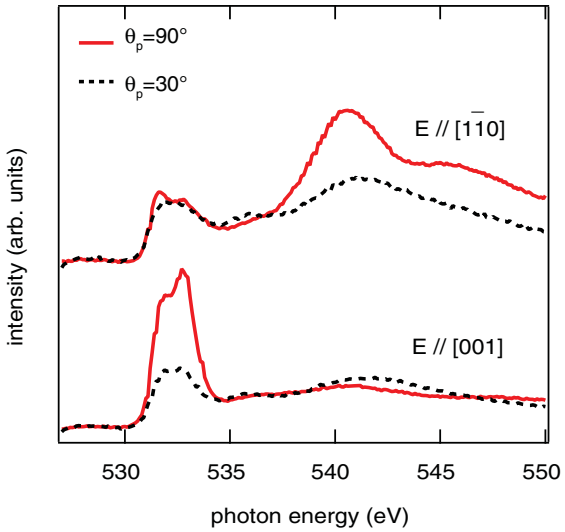

FIG. 3. O K-edge NEXAFS data from uracil deposited onto Cu(110) at room temperature. Spectra are shown for polar two incidence angles (defined, in the standard NEXAFS convention, by the angle θ_p between the surface normal and the principle polarisation vector, **E**, of the radiation), in each of two azimuthal angles.

significantly more intense than that of the lower binding energy (deprotonated) component, perhaps indicating some fractional coverage of intact uracil on the surface. In this regard, too, the data from thymine on Cu(110) show exactly the same effect.[7] The observation of only a single O 1s peak is taken to imply that both oxygen atoms in the molecule inhabit similar (if not identical) bonding environments.

The O K-edge NEXAFS spectra are shown in Fig. 3 for polar incidence angles of 0° (normal incidence) and 60°, corresponding to values of the angle θ_p between the principal polarisation vector **E** and the surface normal of 90° and 30°; these spectra were recorded in each of the two principal azimuths from uracil on Cu(110), after dosing at room temperature. In this case, too, the uracil data are closely similar to those reported for thymine on Cu(110) by Allegretti *et al.*[7] and Furukawa *et al.*,[13] indicating that the orientation of the uracil and thymine molecules on Cu(110) are similar. The spectra are dominated by two features, namely a sharp doublet feature at the absorption edge, and a broader feature at higher energy. The sharp doublet feature is assigned to transitions from the O 1s state to the $\pi^*_{C=O}$ antibonding states; the cross-section for this transition is highest when the polarisation vector of the incident radiation lies perpendicular to the molecular plane, so the fact that this feature is strongest for normal incidence (*E*-vector parallel to the surface) with the *E*-vector lying along [001] indicates that the molecular plane is approximately perpendicular to the surface and lies within the [$\bar{1}$10] azimuth. The angular dependence of the higher-energy peak, assigned to excitations to the $\sigma^*_{C=O}$ resonance for which the cross-section is highest when the polarisation vector is parallel to the molecular plane, is consistent with this interpretation. Notice, though, that the fact that the $\pi^*_{C=O}$ resonance peak does not vanish for normal incidence with the *E*-vector lying along [1$\bar{1}$0], and that the $\sigma^*_{C=O}$ resonance does not vanish for normal incidence with the *E*-vector lying along [001] may indicate that there is some twist and tilt of the molecule relative to this ideal high-symmetry orientation. These residual features, however, may also be attributed to the fact that the incident radiation is not 100% linearly polarised.

A more quantitative estimate of the molecular orientation can be achieved by noting that the intensity of the $\pi^*_{C=O}$ resonance peak must vary as the square of the cosine of the angle between the *E* vector of the incident radiation and the final state π-orbital.[16] In order to obtain this information the four NEXAFS spectra shown in Fig. 3 were therefore fitted with the sum of a sloping background, a step function, and five Gaussian peaks. Two identical Gaussian functions were used to fit the sharp π doublet feature, and three different Gaussian functions were fitted to the broad σ features. Fitting the σ-resonance region of NEXAFS spectra by multiple peaks is of questionable physical significance, but provides a convenient means to achieve more meaningful fits to the much sharper π-resonance peaks; it is the polarisation-angle dependence of only these sharper peaks that we use to extract the molecular orientation. The ratios of the intensities of the doublet features for the four spectra, normalised by the height of the step function, were then used to determine the tilt of the molecule with respect to the surface normal (Θ) and the twist of the molecule with respect to the [$\bar{1}$10]direction of the surface (φ). The two angles were determined to be 10 ± 15° and 15 ± 15°, respectively. Note that for these calculations the degree of polarisation was assumed to be 90%, as reported for this beamline.[6]

The doublet character of the $\pi^*_{C=O}$ resonance seen here is also a feature of the NEXAFS spectra of thymine. It has been seen for thymine adsorbed on Cu(110) in a partially deprotonated form,[7,13] but also in deposited thin films of both thymine and uracil.[17] The doublet has been interpreted as indicative of the inequivalence of the two carbonyl species, resulting from the different environment within the molecular ring occupied by the C(2) and C(4) atoms; as such it is believed to be a feature of the localised NEXAFS final state. This interpretation is consistent with the fact that there is no evidence in any of these studies of a similar spectral splitting in the O 1s SXPS data for which the final state is delocalised in the continuum. Fuji *et al.*[17] actually assign the lower and higher energy π-resonances to the O(7) and O(8) atoms, respectively, but do not explain this assignment. Why the relative intensities of the two components of the doublet should appears to be weakly dependent on the polarisation direction of the incident radiation is unclear, but exactly the same effect is seen in the data recorded from thymine on Cu(110).[7,13]

B. Qualitative analysis of the PhD data

In order to gain quantitative structural information from PhD data it is necessary to compare the experimental spectra with the results of simulations based on realistic multiple scattering calculations for a series of model trial structures, adjusting these structures until a good fit is achieved. However, some aspects of the most probable structures can often be obtained from an inspection of the experimental data. In particular, if a measurement is made in an emission direction

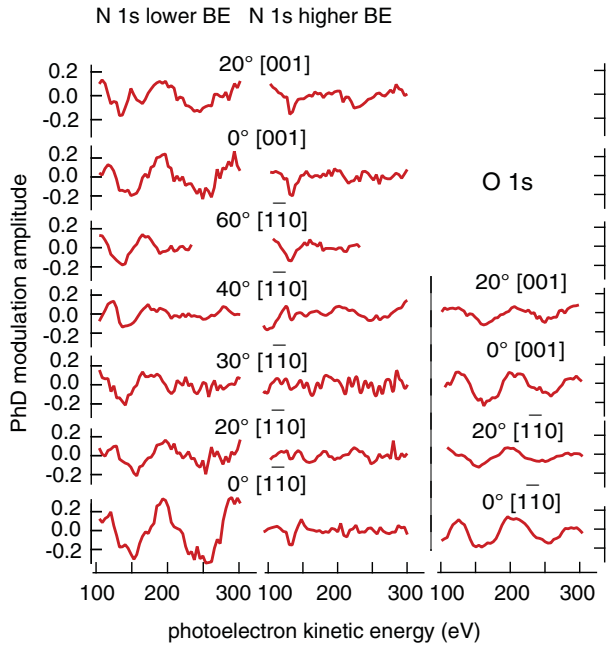

FIG. 4. O 1s and N 1s PhD spectra from uracil deposited onto Cu(110) at room temperature. Shown are the seven N 1s spectra from the higher and lower binding energy peaks seen in Fig. 2(b), and from the four O 1s spectra, that show the largest modulations.

such that there is a strongly scattering nearest neighbour atom in a 180° backscattering position, with respect to the emitter atom and the detector, then the PhD spectrum is commonly dominated by a single periodicity (in electron momentum) with a relatively long period, corresponding to the (short) scattering path-length difference from this one neighbour.[1,2] Figure 4 shows a comparison of the PhD spectra from both the lower and higher binding energy N 1s peaks seen in Fig. 2 in the seven emission directions showing the largest modulation amplitudes, together with the four O 1s PhD spectra showing the strongest modulations. These data were collected from surfaces prepared by deposition of uracil with the Cu(110) substrate at room temperature, with no subsequent annealing. As remarked above, the SXPS from such a preparation shown in Fig. 2 may indicate the presence of some weakly coadsorbed intact uracil. A coadsorbed component of this type is not expected to form strong (short) bonds to the Cu surface, so emission from this species is unlikely to contribute significantly to the observed PhD modulations and will not, of course, have any influence on the PhD spectra from the lower binding energy (deprotonated) N 1s component; it is therefore not considered further in our analysis. The presence of a possible weakly coadsorbed species of this type was deemed to be preferable to a fractional coadsorbate coverage of the fully deprotonated species that is produced by partial annealing.

The PhD spectra of Fig. 4 from the lower binding energy N 1s peak show significantly stronger modulations than those from the higher binding energy peak, while the strongest modulations for both this N 1s component, and the O 1s peak, occur at angles close to normal emission. These dominant long period modulations strongly suggest that both the nitrogen emitter atom with the lower 1s binding energy (attributed on the basis of the SXPS to a deprotonated N in the uracil ring), and at least one of the two oxygen emitter atoms, are sufficiently close to the substrate to be involved in the molecule/surface bonding. Furthermore, we may infer that all these bonding atoms are in atop or near-atop sites. The close similarity of the energies of the main maxima in the normal emission O 1s and (bonding) N 1s PhD spectra also indicates that the Cu–O and Cu–N bondlengths must be quite similar. The fact that the O 1s modulation amplitudes are significantly weaker than those of the N 1s emission could be indicative of either one of two alternative scenarios. One is that only one of the oxygen atoms is bonding to the surface while the other is much further from the surface and thus contributes very little to the PhD modulations due to the weak scattering of the more distant Cu atoms. Alternatively, both oxygen atoms may bond to the surface but either occupy slightly different sites such that their PhD modulations are slightly out of phase, or occupy similar sites that are further displaced from the most symmetric atop sites than those occupied by the bonding nitrogen atom.

The fact that the SXPS shows only a single O 1s peak strongly suggests that the two O atoms have similar bonding environments, favouring a structure in which the uracil bonds to the surface through both O atoms and the (deprotonated) N(3) atom that lies between them. This would also be consistent with the structure found for thymine on Cu(110). On the basis of the preliminary evaluation of our data, however, we cannot formally exclude the possibility that uracil bonds to the surface through only one (O(8)) oxygen atom and the (deprotonated) N(1) atom. Both basic structural models of the uracil/Cu bonding have therefore been explored in our quantitative evaluation of the PhD spectra, as described below.

C. Quantitative analysis of the PhD data

In order to achieve a proper quantitative analysis of the PhD data, multiple scattering simulations for different structural models were performed using the computer codes developed by Fritzsche.[18–20] These are based on the expansion of the final state wave-function into a sum over all scattering pathways that the electron can take from the emitter atom to the detector outside the sample. The level of agreement between the theoretical and experimental modulation amplitudes is quantified using an objective reliability factor (*R*-factor)[1,2] defined and used in a fashion closely similar to that proposed by Pendry for quantitative LEED studies.[21] This *R*-factor is defined such that a value of 0 corresponds to perfect agreement, and a value of 1 to uncorrelated data. The lowest value achievable in practice depends on the complexity of the structure and the amplitude of the modulations, but typically falls in the range 0.2–0.4. Structural models first were tested using a grid-search of structural parameter values. However, due to the large number of structural parameters (creating a multidimensional hyperspace), and inevitable existence of multiple local minima, a heuristic global search algorithm (particle swarm optimisation) proved to be more fruitful.[22] Having located global minima by this approach, an adapted Newton-Gauss algorithm was used to further optimise the structures. In order to estimate the errors associated

TABLE I. Comparison of the structural fitting parameters for thymine on Cu(110) (Ref. 7) cytosine on Cu(110) (Ref. 6) and the N(1)/O(8) and O(7)/N(3)/O(8) bonding models for uracil on Cu(110). It is important to note that, although O(7) and O(8) have been assigned below, it has not been possible to differentiate which O atom is further away from the surface in the O(7)/N(3)/O(8) bonding model of uracil. The four values for the relaxation of the Cu surface atoms perpendicular to the surface, Δz, are with respect to an ideal bulk-terminated structure. z values are distances perpendicular to the surface, xy values parallel to the surface, and d values are interatomic distances.

Parameter	Uracil N(1)/O(8) bonding	Uracil O(7)/N(3)/O(8) bonding	Thymine	Cytosine
z_N (Å)	1.95 ± 0.03	1.94 ± 0.03	1.96 ± 0.02	1.92 ± 0.03
$d_{Cu\text{-}N}$ (Å)	1.96 ± 0.04	1.96 ± 0.04	1.96 ± 0.02	1.94(+0.07/−0.03)
$z_{O(7)}$ (Å)	–	1.90 ± 0.04	2.00 ± 0.03	–
$d_{Cu\text{-}O(7)}$ (Å)	–	1.96 ± 0.04	2.03 ± 0.03	–
$z_{O(8)}$ (Å)	1.89 ± 0.02	1.83 ± 0.04	1.87 ± 0.03	1.90 ± 0.03
$d_{Cu\text{-}O(8)}$ (Å)	1.94 ± 0.02	1.93 ± 0.04	1.91 ± 0.03	1.94(+0.06/−0.04)
φ (°)	6 ± 7	11 ± 5	2 ± 5	12(+7/−12)
Θ (°)	45(+20/−10)	5 ± 20	24 ± 10	10(+20/−10)
Δz_{Cu} (Å)	−0.05 ± 0.05	−0.04 ± 0.05	–	−0.16(+0.06/−0.08)
$\Delta z_{Cu(O(7))}$ (Å)	–	−0.1 ± 0.1	0.05 ± 0.10	–
$\Delta z_{Cu(O(8))}$ (Å)	−0.05 ± 0.03	0.0 ± 0.1	0.05 ± 0.10	−0.04 ± 0.08
$\Delta z_{Cu(N)}$ (Å)	−0.21 ± 0.07	−0.17 ± 0.05	−0.08 ± 0.10	0.00 ± 0.10
Δxy_N (Å)	0.15 ± 0.15	0.25(+0.20/−0.10)	–	0.35 ± 0.50
Δxy_O (Å)	0.4(+0.2–0.4)	O(7) 0.5(+0.4/−0.6) O(8) 0.6(+0.2/−0.6)	–	0.4(+0.2/−0.6)
d_{N-O} (Å)	2.3 ± 0.2	2.3(+0.1/−0.2)	2.3 ± 0.2	2.3 ± 0.3

with the individual structural parameters, we define a variance of the minimum value of the R-factor associated with a best-fit structure, R_{min}.[23] All parameters values giving structures with R-factors less than $R_{min} + Var(R_{min})$ are regarded as falling within one standard deviation of the "best fit" structure. Simulations were performed for the complete set of O 1s and low-binding-energy N 1s PhD spectra (seven N 1s spectra, and four O 1s spectra) shown in Fig. 4, and the global R-factor for these eleven spectra was the parameter minimised in the fitting procedure.

For both the basic models (substrate bonding through the N(1) and O(8) atoms, or bonding through the N(3) and both O atoms) calculations were performed with the adsorbed molecule constrained to retain the intra-molecular bondlengths and bond angles similar to those found in crystalline solid uracil,[24] although small relative displacements of the O and N atoms bonding to the surface were allowed. The (rigid) molecular plane was allowed to tilt by an angle, Θ, from the surface normal, and to twist by an angle, φ, with respect to the $[\bar{1}10]$ azimuth. Both rotations were centred on the bonding N atom which was allowed to vary in height above the surface (z_N)) and to move to off the ideal atop site by an amount (Δxy_N). In order to establish the primary influence of these rotations on the intramolecular scattering, and avoid confusion with the (much greater) influence of changes in the height of the O emitter atoms above the substrate, the bonding oxygen atom(s) was (were) excluded from the Θ rotation. The height of the bonding oxygen atom or atoms above the surface ($z_{O(7)}$ and $z_{O(8)}$) were allowed to vary (independently), as was the distance between the bonding oxygen atom or atoms and the bonding N atom (r_{N-O}); for the O(7)/N(3)/O(8) bonding model these two distances were assumed to be the same. Cu atoms in the outermost substrate layer were allowed to relax perpendicular to the surface, with different values for the Cu atoms that are nearest-neighbours to the bonding atoms of the uracil, ($\Delta z_{Cu(O7)}$, $\Delta z_{Cu(O8)}$, $\Delta z_{Cu(N)}$), and for the remainder of these surface Cu atoms (Δz_{Cu}).

The R-factor values for the best-fit structure for the alternative models involving bonding through the N(1) or the N(3) nitrogen atoms were 0.19 and 0.20, respectively. The Cu–N bondlength in both structures was determined to be 1.96 ± 0.04 Å. For the model involving bonding through the N(1) and O(8) atoms the Cu-O bondlength was determined to be 1.94 ± 0.02 Å while for the model involving substrate bonding through the N(3) atom and both O atoms, Cu-O bondlengths of 1.93 ± 0.04 Å and 1.96 ± 0.04 Å were found. As these are the structural parameters to which the PhD technique is most sensitive, it is reassuring, but also unsurprising, that the two models return very similar bondlengths. The other structural parameter values found for these two alternative models are shown in Table I, together with the comparable values for adsorbed thymine and cytosine on Cu(110). Comparisons of the theoretical and experimental PhD modulations spectra for these two structures, together with schematic representations showing the adsorption geometry, are presented in Figs. 5 and 6.

The difference between these two R-factors (0.01) is significantly smaller than the variance in the lowest value (0.03), so on the basis of this PhD analysis alone, it is not possible to formally exclude either model. However, one further significant difference in the two best-fit structures of Table I is the optimum value of the tilt of the molecular plane away from surface normal, Θ. This parameter has a value of 45 ± (+20/−10)° for the O(8)/N(1) bonding model, and 5 ± 20° for the model involving bonding through the N(3) atom and both O atoms. Only the second of these molecular orientations is consistent with the value obtained from the NEXAFS data of 15 ± 15°. The combination of NEXAFS and PhD results therefore leads us to conclude that the O(8)/N(1) bonding model can be excluded. Note that two other structures

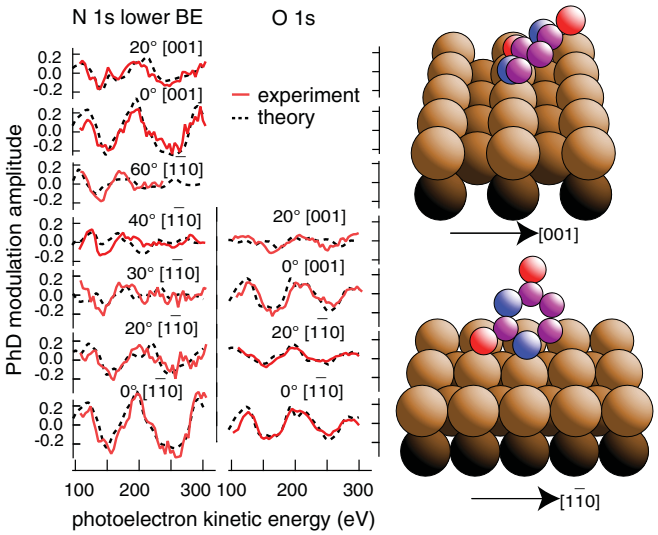

FIG. 5. Comparison of the experimental and theoretical PhD spectra, and schematic representation of the structure, for the best-fit parameters of the N(1)/O(8) bonding model (as listed in Table I). H atoms are omitted from this figure as the results presented here provide no direct information on the location of these atoms. Carbon atoms are represented by the smallest circles, while the nitrogen and oxygen atoms are represented by larger circles that lie in the molecular ring, and outside the molecular ring, respectively.

corresponding to local minima in the *R*-factor structure could also be excluded. Specifically, for the N(1)/O(8) bonding model an alternative solution was found with a tilt of 15 $\pm$ (+10/−5)°, but its *R*-factor of 0.26 falls outside the variance of the best-fit N(3) bonding model. Similarly, a second modification of the N(3) bonding model was found with a *R*-factor of 0.23, just at the limits of the variance, but combined with a significantly larger associated tilt (35 $\pm$ 20°) this solution may also be excluded.

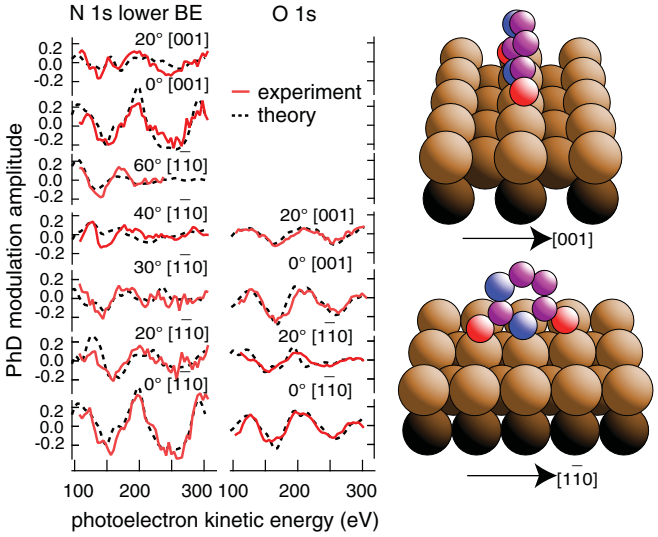

FIG. 6. Comparison of the experimental and theoretical PhD spectra, and schematic representation of the structure, for the best-fit parameters of the N(3)/O(7)/O(8) bonding model (as listed in Table I). H atoms are omitted from this figure as the results presented here provide no direct information on the location of these atoms. Carbon atoms are represented by the smallest circles, while the nitrogen and oxygen atoms are represented by larger circles that lie in the molecular ring, and outside the molecular ring, respectively.

IV. GENERAL DISCUSSION AND CONCLUSIONS

The combination of O 1s and N 1s PhD data, O K-edge NEXAFS, and O 1s and N 1s SXP spectra have provided a clear picture of the structure of uracil chemisorbed on Cu(110), with bonding via both of its oxygen atoms and the N(3) nitrogen atom between, all three of these atoms occupying singly-coordinated off-atop sites relative to nearest-neighbour surface Cu atoms. Perhaps unsurprisingly, this bonding geometry is essentially identical to that of the closely related thymine species on the same surface. Table I shows that the adsorption geometry and chemisorption bondlengths are almost all equivalent to within the precision limits. The one exception is that one of the Cu-O bondlengths is slightly longer for thymine than for uracil, though it is possible this difference stems from slightly different constraints in atom movements allowed in the final refinement of the two structures.

The determined Cu-O (1.93 $\pm$ 0.04 Å and 1.96 $\pm$ 0.04 Å) and Cu-N (1.96 $\pm$ 0.04 Å) bondlengths found for adsorbed uracil are also similar to those for adsorbed cytosine as shown in Table I. The Cu-N bondlength found for uracil (and for thymine and cytosine) is marginally shorter than those found for pyridine (C_5H_5N) [2.00 $\pm$ 0.02 Å (Ref. 25)], 2-methylpyridine ($C_5H_4N(CH_3)$ [2.04 $\pm$ 0.02 Å (Ref. 26)], and ammonia (NH_3) [2.00 $\pm$ 0.04 Å (Ref. 23)] on Cu(110), most probably because the deprotonated N atom in uracil (and thymine and cytosine) can form a stronger Cu–N bond than that associated with the N lone-pair in pyridine and ammonia. On this basis one might expect the Cu–O distance for uracil, thymine and cytosine to be slightly longer than that seen in the dehydrogenated carboxylic acids on Cu(110), and while the associated values for formate (HCOO) [1.90 $\pm$ 0.03 Å (Ref. 27)], acetate (CH_3COO) [1.91 $\pm$ 0.04 Å (Ref. 28)], and benzoate (C_6H_5COO) [1.91 $\pm$ 0.02 Å(Ref. 29)] are smaller, not all of the differences are formally significant when the experimental precision is accounted for.

In many other studies of approximately planar molecules on surfaces the role of intermolecular bonding, particularly through hydrogen bonding, is thought to play an important role in the ordering, and indeed this is the basis of a sub-field based on two-dimensional supramolecular self-assembly. In general, however, these effects have been associated with systems in which the molecules "lie down" on the surface, with the molecular plane approximately parallel to the surface. Indeed, a STM study (without sub-molecular resolution) of uracil on Cu(111) at low temperature (~70 K) (Ref. 30) appeared to identify ordering of molecular trimers that was attributed to this effect. In the present case, however, with the molecular plane perpendicular to the surface, such interactions may be expected to be less important, although in the absence of any evidence of long-range or short-range order in the overlayer, it is not possible to address this issue further. Nevertheless, intermolecular interactions are likely to have far more influence on the ordering of the molecules on the surface (the "self-assembly") than on the local adsorbate-substrate registry, so it is particularly unlikely in the present case that any such interactions have significant impact on the local geometry determined here.

It is interesting to note that the nature of a solid surface imposes quite different constraints on the bonding and chemistry of a molecule like uracil relative to its behaviour in gas or solution phases. When forming its nucleoside, uridine, and in most other N-alkylation reactions, uracil will either react through the N(1) atom, or both the N(1) and N(3) atoms.[31–36] Moreover, to obtain N(3) regioselectivity it is generally necessary to have a protecting group on the N(1) atom.[31,37,38] It has also been shown that in the gas phase the enthalpy of dehydrogenation of these two N atoms differs by ∼0.4 eV, though in polar environments the difference is significantly smaller.[39] At the Cu(110) surface it is evidently the interaction with the N(3) atom that proves to be preferred, but for steric reasons this necessarily also involve interaction of the surface with both O atoms.

ACKNOWLEDGMENTS

The authors acknowledge the partial support of the Engineering and Physical Sciences Research Council (UK) for this work. The computing facilities were provided by the Centre for Scientific Computing of the University of Warwick with support from the Science Research Investment Fund.

[1] D. P. Woodruff and A. M. Bradshaw, Rep. Prog. Phys. **57**, 1029 (1994).
[2] D. Woodruff, Surf. Sci. Rep. **62**, 1 (2007).
[3] N. A. Booth, D. P. Woodruff, O. Schaff, T. Giessel, R. Lindsay, P. Baumgärtel, and A. M. Bradshaw, Surf. Sci. **397**, 258 (1998).
[4] J.-H. Kang, R. L. Toomes, M. Polcik, M. Kittel, J.-T. Hoeft, V. Efstathiou, D. P. Woodruff, and A. M. Bradshaw, J. Chem. Phys. **118**, 6059 (2003).
[5] D. I. Sayago, M. Polcik, G. Nisbet, C. L. A. Lamont, and D. P. Woodruff, Surf. Sci. **590**, 76 (2005).
[6] D. C. Jackson, D. A. Duncan, W. Unterberger, T. J. Lerotholi, D. Kreikemeyer-Lorenzo, M. K. Bradley, and D. P. Woodruff, J. Phys. Chem. C **114**, 15454 (2010).
[7] F. Allegretti, M. Polcik, and D. P. Woodruff, Surf. Sci. **601**, 3611 (2007).
[8] W.-H. Li, W. Haiss, S. Floate, and R. J. Nichols, Langmuir **15**, 4875 (1999).
[9] Q. Chen and N. V. Richardson, Prog. Surf. Sci. **73**, 59 (2003).
[10] M. L. M. Rocco, R. Dudde, K.-H. Frank, and E. E. Koch, Chem. Phys. Lett. **160**, 366 (1989).
[11] A. Martinez, J. Chem. Phys. **123**, 024311 (2005).
[12] K. J. S. Sawhney, F. Senf, M. Scheer, F. Schäfers, J. Bahrdt, A. Gaupp, and W. Gudat, Nucl. Instrum. Methods Phys. Res. A **390**, 395 (1997).
[13] M. Furukawa, H. Fujisawa, S. Katano, H. Ogasawara, Y. Kim, T. Komeda, A. Nilsson, and M. Kawai, Surf. Sci. **532**, 261 (2003).
[14] A. McNutt, Ph.D. dissertation, University of Liverpool, 2002.
[15] A. McNutt, S. Haq, and R. Raval, Surf. Sci. **502**, 185 (2002).
[16] J. Stöhr and R. Jaeger, Phys. Rev. B **26**, 4111 (1982).
[17] K. Fujii, K. Akamatsu, and A. Yokoya, J. Phys. Chem. B **108**, 8031 (2004).
[18] V. Fritzsche, J. Phys.: Condens. Matt. **2**, 1413 (1990).
[19] V. Fritzsche, Surf. Sci. **265**, 187 (1992).
[20] V. Fritzsche, Surf. Sci. **213**, 648 (1989).
[21] J. B. Pendry, J. Phys. C: Solid State Phys. **13**, 937 (1980).
[22] D. A. Duncan, J. Choi, and D. P. Woodruff, "Global search algorithms in photoelectron diffraction structure determination," (unpublished).
[23] N. A. Booth, R. Davis, R. L. Toomes, D. P. Woodruff, C. Hirschmugl, K. M. Schindler, O. Schaff, V. Fernandez, A. Theobald, P. Hofmann, R. Lindsay, T. Giessel, P. Baumgärtel, and A. M. Bradshaw, Surf. Sci. **387**, 152 (1997).
[24] R. F. Stewart and L. H. Jensen, Acta Crystallogr. **23**, 1102 (1967).
[25] T. Giessel, O. Schaff, R. Lindsay, P. Baumgärtel, M. Polcik, A. M. Bradshaw, A. Koebbel, T. McCabe, M. Bridge, D. R. Lloyd, and D. P. Woodruff, J. Chem. Phys. **110**, 9666 (1999).
[26] R. Terborg, M. Polcik, J. T. Hoeft, M. Kittel, M. Pascal, J. H. Kang, C. L. A. Lamont, A. M. Bradshaw, and D. P. Woodruff, Surf. Sci. **457**, 1 (2000).
[27] D. Kreikemeyer-Lorenzo, M. K. Bradley, W. Unterberger, D. A. Duncan, T. J. Lerotholi, and D. P. Woodruff, "Face-dependent bondlengths in molecular chemisorption: the format species on Cu(111) and Cu(110)," Phys. Rev. Lett. (submitted).
[28] K.-U. Weiss, R. Dippel, K.-M. Schindler, P. Gardner, V. Fritzsche, A. M. Bradshaw, A. L. D. Kilcoyne, and D. P. Woodruff, Phys. Rev. Lett. **69**, 3196 (1992).
[29] M. Pascal, C. L. A. Lamont, M. Kittel, J. T. Hoeft, R. Terborg, M. Polcik, J.-H. Kang, R. L. Toomes, and D. P. Woodruff, Surf. Sci. **492**, 285 (2001).
[30] T. Nakagawa, H. Tanaka, and T. Kawai, Surf. Sci. **370**, L144 (1997).
[31] S. Boncel, M. Maczka, and K. Z. Walczak, Tetrahedron **66**, 8450 (2010).
[32] A. P. Martinez and W. W. Lee, J. Org. Chem. **30**, 317 (1965).
[33] A. Alahiane, A. Rochdi, M. Taourirte, N. Redwane, S. Sebti, and H. B. Lazrek, Tetrahedron Lett. **42**, 3579 (2001).
[34] O. D. Gupta, B. Twamley, R. L. Kirchmeier, and J. M. Shreeve, J. Fluorine Chem. **106**, 199 (2000).
[35] S. Boncel, D. Osyda, and K. Z. Walczak, Beilstein J. Org. Chem. **3**, 40 (2007).
[36] K. Yamauchi and M. Kinoshita, J. Chem. Soc. Perkin Trans. 1 **1973**, 391 (1973).
[37] J. T. Kuśmierek and B. Singer, Nucleic Acids Res. **3**, 989 (1976).
[38] A. Gambacorta, M. E. Farah, and D. Tofani, Tetrahedron **55**, 12615 (1999).
[39] M. A. Kurinovich and J. K. Lee, J. Am. Chem. Soc. **122**, 6258 (2000).